Reactions of Unsaturated Nickel–Tungsten and Nickel–Molybdenum Complexes with Organic Disulfides. Synthetic and Structural Studies

Aaron F. Bartlone,[†] Michael J. Chetcuti,*[,†] Phillip E. Fanwick,[‡] and Kenneth J. Haller[†]

Department of Chemistry and Biochemistry, University of Notre Dame, Notre Dame, Indiana 46556, and Department of Chemistry, Purdue University, West Lafayette, Indiana 47907

Received August 6, 1992

The behavior of the unsaturated complex (η-C_5Me_5)Ni–W(CO)$_3$(η-C_5H_4Me) (Ni–W, **1**) toward selected chalcogenide-containing ligands is described. The Ni–W species is inert to Me_2S under ambient reaction conditions, but disulfides and diselenides react with **1**. Diphenyl disulfide, dimethyl disulfide, and diphenyl diselenide oxidatively add across the mixed-metal bond to afford (η-C_5Me_5)Ni(μ-CO)(μ-ER)W(CO)(ER)(η-C_5H_4Me) (Ni–W; ER = SPh, SMe, SePh), which contain bridging and terminal thiolate or selenate ligands. A similar Ni–Mo product was formed when (η-C_5Me_5)Ni–Mo(CO)$_3$(η-C_5H_4Me) was treated with PhS_2Ph. In most cases the reactions are clean, but [(η-C_5Me_5)Ni(μ-SePh)]$_2$ was also isolated in the diphenyl diselenide reaction. All the complexes are fluxional on the NMR time scale. The bis(benzenethiolate) nickel–tungsten species was studied by VT ^{1}H NMR: some dynamic behavior was arrested at −80 °C. Structures of (η-C_5Me_5)Ni(μ-CO)(μ-SPh)W(CO)(SPh)(η-C_5H_4Me) (Ni–W, **2a**) and [(η-C_5Me_5)Ni(μ-SePh)]$_2$ (**3**) were ascertained by single-crystal X-ray diffraction studies. Crystal data for $C_{30}H_{32}O_2NiS_2W$ (**2a**): monoclinic, $P2_1/c$ (No. 14), a = 15.101(1) Å, b = 11.531(2) Å, c = 17.262(2) Å, β = 108.01(1)°, Z = 4. Crystal data for $C_{32}H_{40}Ni_2Se_2$ (**3**): triclinic, $P\bar{1}$ (No. 2), a = 8.444(4) Å, b = 9.495(3) Å, c = 10.851(6) Å, α = 112.64(3)°, β = 108.88(4)°, γ = 95.92(3)°, Z = 1.

Introduction

The chemistry of transition metal complexes with chalcogenide containing ligands has undergone a renaissance in recent years. The diverse bonding modes exhibited by molecules containing sulfur and other group 16 elements with transition metals and the breadth of unusual structures obtained with chalcogenide-containing ligands has kindled interest among many research groups. In the bioinorganic field there is topical interest in transition metal sulfur chemistry: nitrogenase enzymes are believed to contain Fe–Mo–S cluster cores,[1] and various metalloenzymes and other biochemically important molecules such as ferredoxins and hydrogenases contain sulfur–transition metal active sites. The importance of nickel in bioinorganic systems[2] (frequently exhibiting interactions with sulfur) is increasingly being recognized.[2-4] Molybdenum or tungsten catalysts, dispersed on alumina and promoted by cobalt or nickel salts, are the principal metals used in the HDS process that chemically extracts the sulfur from petroleum gases.[5]

The discovery of the coordinatively unsaturated mixed-metal species (η-C_5Me_5)Ni–M(CO)$_3$(η-C_5H_4Me) (Ni–M: **1**, M = W; **1′**, M = Mo)[6] in our laboratories led us to investigate reactions of these molecules with unsaturated hydrocarbon ligands and with various two-electron-donor ligands. These studies address the chemistry of **1** and **1′** with ligands containing elements from groups 14 and 15 of the periodic table and remain in progress.[7] The metals present in **1** and **1′** are pertinent to the bioinorganic and catalytic systems cited earlier. As an entry into the chemistry of group 16 ligands with these unsaturated metal–metal-bonded complexes, we have initiated a study of their chemistry with simple chalcogenide-containing ligands. Herein we present the chemistry of **1** with the ligands Me_2S, PhS_2Ph, $PhSe_2Ph$ and MeS_2Me.

Results

Reaction of (η-C_5Me_5)Ni–W(CO)$_3$(η-C_5H_4Me) with Me_2S. We attempted to react Me_2S with the complex (η-C_5Me_5)Ni–W(CO)$_3$(η-C_5H_4Me) (**1**), in order to study the coordination properties of a simple sulfur-containing ligand. We were surprised to discover that toluene solutions of **1** do not react with dimethyl sulfide under ambient conditions or when heated. Slow deposition of a sparingly soluble dark precipitate resulted when solutions of **1** were refluxed with ethereal solutions of dimethyl sulfide over a 2 day period. When **1** is themolyzed in solution, decarbonylation and clustering result to afford the sparingly soluble species $Ni_2W_2(CO)_4(\eta$-$C_5Me_5)_2(\eta$-$C_5H_4Me)_2$: this species is the likely decomposition product.

Reaction of (η-C_5Me_5)Ni–M(CO)$_3$(η-C_5H_4Me) (M = Mo, W) with PhS_2Ph. Complex **1** reacts rapidly with PhS_2Ph at −78 °C. The deep blue color of **1** was discharged instantaneously on addition of the reagent and a brown solution resulted. IR spectra of the crude reaction mixture revealed two new ν(CO) bands. An attempt to purify the species via silica gel chromatography was unsuccessful as the compound was immobile on a silica gel column. The product of this reaction was isolated and purified in good yield by filtration of the crude reaction mixture and crystallization. No other products were isolated: if these are present, they are formed in low yield.

The empirical formula (η-C_5Me_5)NiW(CO)$_2$(η-C_5H_4Me)(SPh)$_2$ was established for the reaction product **2a** by spectroscopic methods; some of these data are tabulated (Tables I, II). The complex exhibits resonances for η-C_5Me_5, η-C_5H_4Me

[†] University of Notre Dame.
[‡] Purdue University.

(1) (a) Orme-Johnson, W. H. *Annu. Rev. Biophys. Biophys. Chem.* **1985**, *14*, 419 and cited references. (b) Nelson, M. J.; Levy, M. A.; Orme-Johnson, W. H. *Proc. Natl. Acad. Sci. U.S.A.* **1983**, *80*, 147.
(2) *The Bioinorganic Chemistry of Nickel*; Lancaster, J. R., Ed.; VCH Publishers: New York, 1988; see also cited references.
(3) (a) Maroney, M. J.; Colpas, G. J.; Babyinka, C. *J. Am. Chem. Soc.* **1990**, *112*, 7067. (b) Hausinger, R. P. *Microbiol. Rev.* **1987**, *51*, 122.
(4) Cotton, F. A.; Wilkinson, G. *Advanced Inorganic Chemistry*, 5th ed.; John Wiley and Sons: New York, 1988; Chapter 30, p 1375 and cited references.
(5) For a recent review of thiophene complexes and their relation to HDS catalysis see: Angelici, R. J. *Acc. Chem. Res.* **1988**, *21*, 388.
(6) Chetcuti, M. J.; Grant, B. E.; Fanwick, P. E.; Geselbracht, M. J.; Stacy, A. M. *Organometallics* **1990**, *9*, 1343.
(7) (a) Chetcuti, M. J.; Grant, B. E.; Fanwick, P. E. *Organometallics* **1990**, *9*, 1345. (b) Chetcuti, M. J.; Deck, K. J.; Fanwick, P. E.; Gordon, J. C.; Grant, B. E. *Organometallics* **1992**, *11*, 2128.

0020-1669/93/1332-1435$04.00/0

Table I. IR and Analytical Data

complex	ν(CO) (cm^{-1})	empirical formula	calcd (expt) % C	calcd (expt) % H
2a[a]	1950(s), 1891(w), 1761(m)	$NiWC_{30}H_{32}O_2S_2$	49.28 (48.68)	4.41 (4.79)
2a'[b]	1945(s), 1890(w), 1745(m)	$NiMoC_{30}H_{32}O_2S_2$	56.01 (55.70)	5.01 (5.21)
2b[c]	1938(s), 1892(w), 1750(m)	$NiWC_{30}H_{32}O_2Se_2$	43.67 (43.69)	3.91 (4.00)
2c[a]	1948(s), 1752(m)	$NiWC_{20}H_{28}O_2S_2$	39.60 (39.57)	4.66 (4.65)
3[a]		$Ni_2C_{32}H_{40}Se_2$	54.86 (54.91)	5.78 (5.76)

[a] Hexanes. [b] CH_2Cl_2. [c] Nujol mull.

Table II

(a) ^{1}H NMR Data[a]

complex	C_5Me_5	C_5H_4Me	C_5H_4Me[b]	*R*
2a	1.83	1.87	4.86, 4.93	7.42, 7.17, 7.07
2a[c]	1.75	1.70	4.57, 5.01, 5.28, 5.79	7.46, 7.31, 7.26, 7.08, 6.88
2a'	1.77	1.67	4.80, 4.74	7.47, 7.15, 7.10
2b	1.85	1.75	4.76, 4.89	7.54, 7.16, 7.14
2c	1.78	1.84	5.20, 5.30	2.16
3	1.80			7.50, 7.25

(b) ^{13}C NMR Data[a,d]

complex	C_5Me_5	C_5Me_5	C_5H_4Me	C_5H_4Me	*R*
2a	8.9	104.7	12.3	91.9, 92.8, 109.5 [C(1)]	124.9, 127.3, 132.2
2a[c]	9.3	104.5	12.3	88.6, 92.5, 93.1, 93.9, 114.6 [C(1)]	122.9, 127.3, 128.1, 128.2, 129.4, 132.2, 133.1
2a'	9.0	105.1	12.5	93.8, 95.7, 105.3 [C(1)]	124.9, 127.8, 132.8
2b	9.5	105.0	12.4	90.5, 91.8, 106.0 [C(1)]	125.9, 128.3, 134.1

[a] Chloroform-d_1; all values in ppm. All signals except Me groups are multiplets in ^{1}H NMR. [b] $[AB]_2$ spin system (pseudotriplets). [c] At −80 °C in acetone-d_6. C_5H_4Me appear as ABCD type multiplets in ^{1}H NMR. [d] CO's (except for **2a** at 217.0 ppm) and Ph ipso carbons not seen.

and Ph protons in its ^{1}H NMR spectrum in a 1:1:2 ratio respectively. Aromatic resonances of the η-C_5H_4Me ligand appear as an $[AB]_2$ spin system, indicating that a mirror plane bisects the molecule on the ^{1}H NMR time scale. Though signal integration established that two Ph resonances are present, only one set of resonances (appearing as three multiplets) is observed at ambient temperatures. These symmetry and molecular data are corroborated by the ^{13}C NMR spectrum of **2a**.

The IR data for **2a** reveal ν(CO) stretches whose frequencies correspond to both a terminal CO ligand and a bridging CO group (and a weak third absorption). Microanalytical data are consistent with the empirical formulation of **2a** as (η-C_5Me_5)NiW(CO)$_2$(η-C_5H_4Me)(SPh)$_2$. This is corroborated by the FAB MS data which shows the parent ion with its expected isotopic envelope.

The complex (η-C_5Me_5)Ni–Mo(CO)$_3$(η-C_5H_4Me) (**1'**), a nickel–molybdenum analog of **1**, reacts similarly with PhS_2Ph. A species of empirical formula (η-C_5Me_5)NiMo(CO)$_2$(η-C_5H_4Me)(PhS_2Ph) (**2a'**) was isolated from this reaction. Spectroscopic data for **2a'** parallel those of **2a**, and suggest the two species are isostructural.

Reaction of 1 with $PhSe_2Ph$. The oxidative addition of disulfides to **1** may be extended to organic diselenides. An immediate reaction ensued when diphenyl diselenide was added to a solution of **1** at −78 °C. In contrast to the PhS_2Ph reaction, two species were isolated upon work up. The primary product was a brown complex that resembled **2a** in its spectroscopic properties. IR and ^{1}H and ^{13}C NMR spectra of this species mirror those of its sulfur analog (Tables I, II). The ^{77}Se NMR spectrum for **2b** exhibited a single resonance at +1045 ppm (relative to Me_2Se),[8] that is not too different from the value of +923 ppm noted for the bridging SePh groups in the anion $[W_2Cl_6(\mu\text{-SePh})_2(\mu\text{-Se})]^{2-}$.[9] The spectrum of **2b** showed that only one type of selenium atom was present on the ^{77}Se NMR time scale, but the low signal to noise ratio of this singlet precluded the observation of any ^{183}W–^{77}Se satellites. These data, in conjunction with microanalyses results and MS data indicate that the complex can be formulated as (η-C_5Me_5)NiW(CO)$_2$(η-C_5H_4Me)(SePh)$_2$ (**2b**), the benzeneselenate analog of **2a**.

Chart I

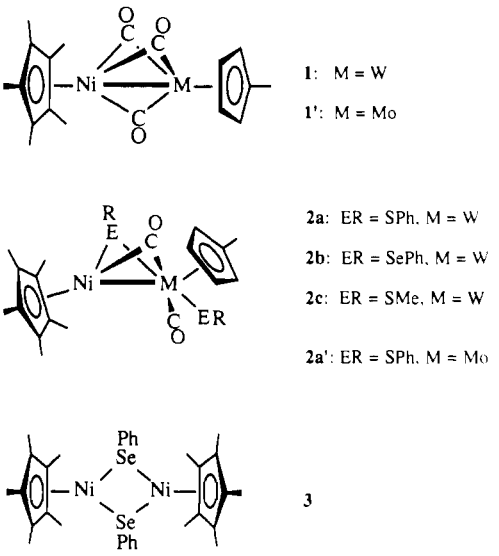

Small quantities of another species (**3**) were also isolated. IR spectroscopy indicated a lack of carbonyl ligands for this compound while NMR data revealed that **3** contained η-C_5Me_5 and Ph ligands in a 1:1 ratio. The absence of η-C_5H_4Me groups implied that no tungsten was present in the molecule:[10] MS data support the formulation of this species as $[Ni(\eta\text{-}C_5Me_5)(SePh)]_2$ (**3**). A single crystal X-ray diffraction study, discussed later in this article, confirmed the proposed structure of **3** to be that shown in Chart I. Similar $[Ni(\eta\text{-}C_5H_5)(\mu\text{-SR})]_2$ species have

(8) Measured using $PhSe_2Ph$ as an external reference: $\delta(PhSe_2Ph)$ = 453 ppm relative to Me_2Se. See: Dean, P. A. W.; Vittal, J. J.; Payne, N. C. *Inorg. Chem.* **1987**, *26*, 1683.

(9) Ball, J. M.; Boorman, P. M.; Fait, J. F.; Kraatz, H.-B.; Richardson, J. F.; Collison, D.; Mabbs, F. E. *Inorg. Chem.* **1990**, *29*, 3290.

(10) Metal–Cp or –Cp' bonds are strong and nonlabile. They are rarely cleaved under normal conditions. One of the few well-established counterexamples is given in: Casey, C. P.; O'Connor, J. M.; Haller, K. J. *J. Am. Chem. Soc.* **1985**, *107*, 1241.

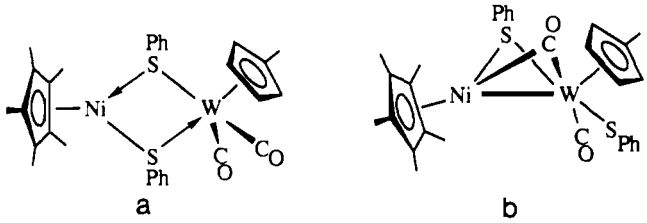

Figure 1. Two possible structures for $NiWCp^*Cp'(SPh)_2(CO)_2$ (**2a**). b is the actual structure adopted.

been prepared in the 1960s[11] and 1970s[12] by reacting nickelocene with thiols. Photolysis of $[Ni(\eta\text{-}C_5H_5)(\mu\text{-}CO)]_2$ with disulfides also affords $[Ni(\eta\text{-}C_5H_5)(\mu\text{-}SR)]_2$ species.[13]

We speculated that traces of $[Ni(\eta\text{-}C_5Me_5)(\mu\text{-}CO)]_2$, sometimes present in samples of "pure" **1**, might be the source of **3**. However, under the same experimental conditions that lead to formation of **2b** and **3**, we have demonstrated that $[Ni(\eta\text{-}C_5Me_5)(\mu\text{-}CO)]_2$ does not react with $PhSe_2Ph$. Furthermore, complex **2a** does not appear to be the source of **3** as no decomposition products can be detected when sealed solutions of **2a** are maintained at ambient temperatures for periods of up to 1 week. These results establish that **3** is derived from the heterobimetallic species **1**, and not from **2a**. Significant quantities of $[W(CO)_3(\eta\text{-}C_5H_4Me)]_2$ are also formed concurrently with **3**. The ditungsten complex, a common minor product in reactions of **1**, was identified by its color and its IR spectrum and was discarded.

Reaction of 1 with MeS_2Me. The reaction of **1** with MeS_2Me followed a pathway reminiscent of the reactions of PhS_2Ph described previously. However, this reaction is more vigorous than that of its diphenyl disulfide analog. Large quantities of decomposition products were obtained and we were unable to isolated any pure compound at ambient temperatures. The species $[W(CO)_3(\eta\text{-}C_5H_4Me)]_2$ was again identified spectroscopically. There is NMR evidence that the homobimetallic nickel complex $[Ni(\eta\text{-}C_5Me_5)(\mu\text{-}SMe)]_2$ analogous to complex **3** may be formed but this species, if present, could not be isolated. Significant quantities of a heterobimetallic product were only isolated from the reaction of **1** with MeS_2Me at −78 °C and in moderate yield. The product appears to be $(\eta\text{-}C_5Me_5)Ni\text{-}W(CO)_2(\eta\text{-}C_5H_4Me)(SMe)_2$ (**2c**). All spectroscopic data are in accord with this formulation.

Structures of the Bis(thiolate) Complexes 2a′ and 2a–c. Dialkyl disulfide ligands generally react with dinuclear metal complexes through cleavage of the disulfide bond, oxidative addition of the two thiolate ligands to the metal centers and concomitant metal–metal bond cleavage. Two feasible structures that are in accord with the spectroscopically obtained molecular formula for **2a** are depicted in Figure 1.

In the structure represented by Figure 1a, benzenethiolato ligands bridge the dimetal center, acting as three-electron donors. Electron-counting arguments for the structure represented in Figure 1a imply that no metal–metal bond exists here. A mirror plane is either present in this structure or is readily available in principle (if the phenyl groups are not related by a mirror plane, rapid inversion of the pyramidal chalcogen atoms is also necessary). This structure would then be in accord with the NMR data for **2a**. It is at odds with IR spectral data that indicate that both a terminal and a bridging carbonyl ligand are present in this species.

The second viable structure shown (Figure 1b) agrees with IR data. This depiction contains two bridging ligands—a benzenethiolato group and a μ-CO group. The second benzenethiolato ligand in the molecule is terminally ligated to the tungsten atom. As **1** can be regarded as having Ni–W double bond character, a Ni–W bond may be retained in **2a** even if oxidative addition of two RS fragments to **1** occurs. This structure can be reconciled with the NMR data if a fluxional process interconverts bridging and terminal SPh groups *and* bridging and terminal CO groups.

In order to establish the structure of complexes **2**, an X-ray diffraction study of a molecule in this class was desired. An X-ray structural analysis was carried out on a single crystal of **2a**. Cell and data collection parameters, atomic positional parameters, and key bond lengths and bond angles are collected in Tables III–V respectively. A labeled ORTEP plot is shown in Figure 2.

Complex **2a** can be represented as $(\eta\text{-}C_5Me_5)Ni(\mu\text{-}CO)(\mu\text{-}SPh)W(CO)(SPh)(\eta\text{-}C_5H_4Me)$ (Ni–W) and corresponds to the structure portrayed in Figure 1b. The molecule contains a

Table III. Key Cell and Data Collection Parameters for **2a** and **3**

	2a	**3**
formula	$NiWC_{30}H_{32}O_2S_2$	$Ni_2C_{32}H_{40}Se_2$
fw	731.26	700.00
a (Å)	15.101(1)	8.444(4)
b (Å)	11.531(2)	9.495(3)
c (Å)	17.262(2)	10.851(6)
α (deg)		112.64(3)
β (deg)	108.010(8)	108.88(4)
γ		95.92(3)
V (Å^3)	2858(1)	733.4(15)
Z	4	1
space group	$P2_1/c$ (No. 14)	$P\bar{1}$ (No. 2)
T (°C)	20 ± 1	−147 ± 2
λ (Å)	0.710 73	0.710 73
ρ_{calc} (g cm^{-3})	1.699	1.58
μ (cm^{-1})	49.35	37.7
$R(F_o)^a$	0.029	0.057
$R_w(F_o)^b$	0.034	0.066

^{a} $R(F_o) = \Sigma|F_o - F_c|/\Sigma|F_o|$. ^{b} $R_w(F_o) = (\Sigma w(F_o - F_c)^2/\Sigma wF_o^2)^{1/2}$.

Table IV. Atomic Positional Parameters for Key Non-Hydrogen Atoms of **2a** with Esd's in Parentheses

atom	x	y	z
W	0.18789(2)	0.13871(3)	0.14718(2)
Ni	0.32419(6)	0.1416(1)	0.08475(6)
S(1)	0.1836(1)	0.1590(2)	0.0037(1)
S(10)	0.1509(2)	−0.0575(2)	0.0834(1)
O(17)	0.3371(5)	0.0314(7)	0.2971(4)
O(21)	0.3345(4)	0.3388(5)	0.1855(4)
C(1)	0.1590(5)	0.3071(8)	−0.0246(5)
C(11)	0.1790(5)	−0.1774(8)	0.1477(6)

Table V. Important Bond Lengths (Å) and Bond Angles (deg) for $(\eta\text{-}C_5Me_5)Ni(\mu\text{-}CO)(\mu\text{-}SPh)W(CO)(SPh)(\eta\text{-}C_5H_4Me)$ (Ni–W, **2a**) with Esd's in Parentheses

		Distances	
W–S(1)	2.469(2)	W–S(10)	2.503(2)
W–C(17)	1.97(1)	W–C(21)	2.01(1)
Ni–S(1)	2.160(2)	Ni–C(21)	1.970(9)
S(1)–C(1)	1.784(9)	S(10)–C(11)	1.74(1)
O(17)–C(17)	1.15(1)	O(21)–C(21)	1.20(1)
W–Ni	2.602(1)		
Ni–C(Cp*)	2.11	W–C(Cp′)	2.309
		Angles	
Ni–W–S(1)	50.34(5)	Ni–W–S(10)	85.82(6)
Ni–W–C(17)	82.5(3)	Ni–W–C(21)	48.5(3)
S(1)–W–S(10)	73.21(8)	S(1)–W–C(17)	129.9(3)
S(1)–W–C(21)	78.7(3)	S(10)–W–C(17)	89.4(3)
S(10)–W–C(21)	134.1(3)	C(17)–W–C(21)	81.5(4)
W–Ni–S(1)	61.64(6)	W–Ni–C(21)	49.9(3)
S(1)–Ni–C(21)	87.7(3)	W–S(1)–Ni	68.02(7)
W–S(1)–C(1)	107.7(3)	Ni–S(1)–C(1)	110.2(3)
W–S(10)–C(10)	117.4(3)	W–C(17)–O(17)	175.5(9)
W–C(21)–Ni	81.6(4)	W–C(21)–O(21)	152.7(8)
Ni–C(21)–O(21)	125.6(7)		

(11) Schropp, W. K. *J. Inorg. Nucl. Chem.* **1963**, *24*, 1688.
(12) (a) Ellgen, P. C.; Gregory, C. D. *Inorg. Chem.* **1971**, *10*, 980. (b) Hirabayashi, T. *J. Organomet. Chem.* **1972**, *39*, C85.
(13) Davidson, J. L.; Sharp, D. W. A. *J. Chem. Soc., Dalton Trans.* **1973**, 1957.

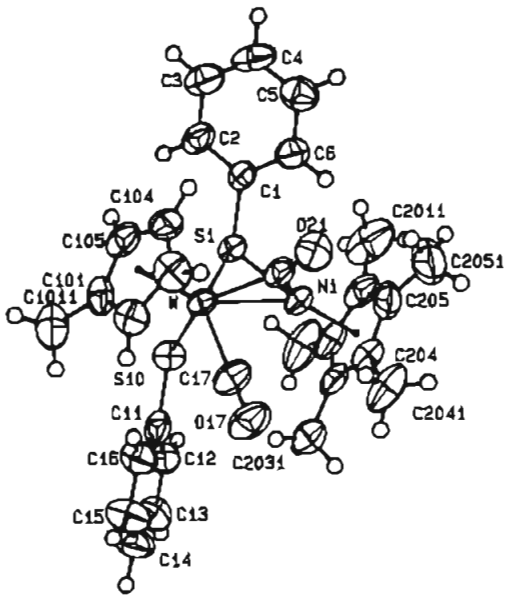

Figure 2. Labeled ORTEP plot of $(\eta\text{-}C_5Me_5)Ni(\mu\text{-}CO)(\mu\text{-}SPh)W(CO)(SPh)(\eta\text{-}C_5H_4Me)$ (Ni–W, **2a**). Ellipsoids are shown at the 50% probability level for all atoms except hydrogen.

normal[14] Ni–W single bond of 2.602(1) Å and has a butterfly-type $NiW(\mu\text{-}SPh)(\mu\text{-}CO)$ core, similar to that observed in the $\mu\text{-}CH_2$ species $(\eta\text{-}C_5Me_5)Ni(\mu\text{-}CO)(\mu\text{-}CH_2)W(CO)_2(\eta\text{-}C_5H_5)$ (Ni–W).[7] The dihedral angle between the Ni–S_μ–W and Ni–C_μ–W planes is 113° (cf. 109° in the methylene complex). Both sulfur atoms are in nonlinear geometries [W–S–C_{Ph} = 117.4(3)°; W–S_μ–C_{Ph} = 107.7(3)°; Ni–S_μ–C_{Ph} = 110.2(3)°], and the sum of the angles around S_μ equals 286°. The two dienyl groups are in a trans conformation relative to each other, while the two SPh and the two carbonyl ligands are in a mutually cis conformation respectively.

The W–S_μ distance is significantly shorter than the terminal W–S bond length [2.469(2) and 2.503(2) Å respectively]. Recently reported W–S distances for μ-thiolate sulfur bonds include 2.429(5) Å in $[W_2Cl_6(\mu\text{-}SEt)(\mu\text{-}SEt_2)_2]^-$ and 2.446(4) Å in $[W_2Cl_6(\mu\text{-}SC_4H_8Cl)(THT)_2]^-$.[15] The Ni–$S_\mu$ distance of 2.160(2) Å is short compared to other reported Ni–$(SR)_\mu$ bonds: values for Ni–$(SR)_\mu$ distances observed in homoleptic $[Ni_2(\mu\text{-}SR)_2(SR)_4]^{2-}$ species are 2.220(2), 2.212(1) Å [R = $p\text{-}C_6H_4Cl$][16] and 2.215 (av), 2.225 (av) Å [R = Et];[17] a mean value of 2.30 Å was noted for the six Ni–$(SR)_\mu$ bonds in $[Ni_2(\mu\text{-}SR)_3(SR)_2]^-$ (R = 2,4,5-^{i}Pr$_3$C$_6$H$_2$).[18] Reported Ni–$(SR)_\mu$ bond lengths in $Ni(terpy)(\mu\text{-}SPh)(SPh)]_2$ are 2.410(2) and 2.519(2) Å.[19]

The solid-state structure of **2a** corresponds to the observed IR spectrum of this species. It is at odds with its symmetry in solution as deduced by NMR spectroscopy. A fluxional process in **2a** may generate a mirror plane that effectively bisects the $\eta\text{-}C_5H_4Me$ ligand and render the two Ph groups equivalent on the NMR time scale. Such a process may be arrested at low temperature and the molecule would now exhibit a lower effective symmetry in its NMR spectrum. Low-temperature ^1H and ^{13}C NMR spectra of **2a** were obtained to test this hypothesis.

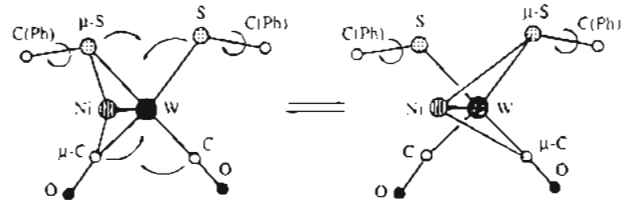

Figure 3. Identical Molecular Editor plots of the core of **2a** showing the proposed fluxional process. Relatively little atomic motion (indicated by arrows) is required to effect the bridge–terminal exchange of SPh groups and of CO groups, respectively, needed to generate an effective mirror plane on the NMR time scale. Rotation about the S–C_{Ph} bonds is also shown. Cp*, Cp′, and Ph ring carbon atoms except the ipso carbons are omitted for clarity.

Low-Temperature NMR Spectra of $(\eta\text{-}C_5Me_5)Ni(\mu\text{-}CO)(\mu\text{-}SPh)W(CO)(SPh)(\eta\text{-}C_5H_4Me)$ (Ni–W, 2a). Observations. A sample of **2a** was dissolved in acetone-d_6 and the sample was cooled from +20 to −40 °C in the NMR spectrometer. There was little apparent change in the spectrum of **2a** until the lower limit of this range was approached. Below −40 °C, the three Ph proton multiplets and the two (pseudotriplet) $[AB]_2$ aromatic $\eta\text{-}C_5H_4Me$ resonances broadened and collapsed. By −80 °C, four broad multiplets were discernible for the $\eta\text{-}C_5H_4Me$ aromatic protons and numerous overlapping multiplets were observed in the Ph region of the ^1H NMR spectrum. No further sharpening of the resonances ensued as the temperature was lowered further to −95 °C in three steps. (Viscosity-induced broadening and/or sample precipitation may counteract the narrower line width expected with a closer approach to the low-temperature limiting spectrum.) Using an approximate coalescence temperature of −60 ± 5 °C led to an estimate of $\Delta G^\ddagger = 40.6 \pm 2$ kJ/mol for the free energy of activation of the arrested dynamic process.[20]

While the overlapping Ph proton signals are not readily interpretable in the ^1H NMR spectrum, the four distinct multiplets noted for the $\eta\text{-}C_5H_4Me$ aromatic resonances at −80 °C indicate that the molecule now lacks an effective mirror plane of symmetry: these signals appear as an ABCD spin system. The ^{13}C NMR spectrum of **2a** at −80 °C mirrors these spectral data. Five aromatic $\eta\text{-}C_5H_4Me$ signals and seven distinct Ph resonances are discernible.

Dynamic Process in 2a. The low-temperature spectra noted are in accord with the solid-state structure of **2a**. Many dynamic processes are operative in complex **2a**, only some of which are arrested as the temperature is lowered to −80 °C. Two mechanisms that can explain the appearance of the NMR spectra of **2a** are (1) rapid pairwise exchange between bridging and terminal SPh ligands, coupled with simultaneous bridge–terminal carbonyl ligand exchange, and (2) rotation about the S–C_{Ph} axes. (The possibility of a third process—(3) inversion at sulfur—is addressed at the end of this section.) Processes 1 and 2 can explain the ambient-temperature spectra of **2a**. This dynamic behavior (shown in Figure 3) would generate an effective mirror plane of symmetry on the ^1H NMR time scale that would bisect the two Ni–W–S_μ planes *and* the two Ni–W–C_μ planes, and would render the two SPh groups equivalent on the NMR time scale. The carbonyl ligands, undergoing rapid site exchange, would also be symmetry related to each other. Little motion of the $\eta\text{-}C_5H_4Me$ ligand would be needed to allow it to be bisected by this mirror plane, resulting in an $[AB]_2$ type spectrum being observed for the aromatic protons of this ligand.

This dynamic behavior is similar to that proposed for the μ-methylene complex $(\eta\text{-}C_5Me_5)Ni(\mu\text{-}CO)(\mu\text{-}CH_2)W(CO)_2(\eta\text{-}$

(14) Most nickel–tungsten single bonds span the 2.64 ± 0.05 Å range: Chetcuti, M. J.; Fanwick, P. E.; Gordon, J. C.; Green, K. A.; Morgenstern, D. *Organometallics* **1989**, *8*, 1790 and cited references.
(15) Boorman, P. M.; Gao, X.; Fait, J. F.; Parvez, M. *Inorg. Chem.* **1991**, *30*, 3886.
(16) Colpas, G. J.; Kumar, M.; Day, R. O.; Maroney, M. J. *Inorg. Chem.* **1990**, *29*, 4779.
(17) Watson, A. D.; Rao, C. P.; Dorfman, J. R.; Holm, R. H. *Inorg. Chem.* **1985**, *24*, 2820.
(18) Silver, A.; Millar, M. *J. Chem. Soc., Chem. Commun.* **1992**, 948.
(19) Baidya, N.; Olmstead, M.; Mascharak, P. K. *Inorg. Chem.* **1991**, *30*, 929.
(20) This value is obtained from analysis of the Cp′ aromatic resonances using a formula strictly applicable only to a two-site exchange process with no coupling present. Errors introduce by ignoring coupling are likely to be swamped by the large uncertainty in the coalescence temperature: Gutowsky, H. S.; Holm, C. H. *J. Chem. Phys.* **1956**, *25*, 1228.

Table VI. Atomic Positional Parameters for Key Independent Non-Hydrogen Atoms of **3** with Esd's in Parentheses

atom	x	y	z
Ni	0.095 99(7)	0.637 39(6)	0.163 98(5)
Se	−0.012 90(6)	0.634 29(5)	−0.061 11(4)
C(11)	0.194 3(6)	0.682 0(5)	−0.094 9(4)

Table VII. Key Atomic Distances (Å) and Bond Angles (deg) for $[(\eta\text{-}C_5Me_5)Ni(\mu\text{-}SePh)]_2$ (**3**) with Esd's in Parentheses[a]

Distances			
Ni–Se	2.301(1)	Ni–Se	2.301(1)
Ni–Ni′	3.216(1)	Se–Se′	3.292(1)
Se–C(11)	1.945(3)	Ni–C(Cp*)	2.112
Angles			
Ni–Se–Ni′	88.66(2)	Ni–Se–C(11)	103.16(9)
Ni′–Se–C(11)	104.4(1)	Se–Ni–Se′	91.34(2)

[a] Coordinates of primed atoms are related to corresponding unprimed atoms by the symmetry transformation A′(x, y, z) = A(−x, 1 − y, −z).

C_5H_5) (Ni–W).[7b] However only one set of ligands (the mutually trans carbonyl groups that are each cis to the bridging methylene ligand) are involved in bridge–terminal exchange in the methylene complex. In **2a**, both the bridging and terminal carbonyl ligands *and* the bridging and terminal SPh ligands respectively are simultaneously undergoing mutual site exchange.

Rapid rotation about the S–C_{Ph} bond (process 2) makes the two ortho protons of the Ph group equivalent, and by virtue of the effective mirror plane present, symmetry related to the other set of two ortho protons on the other SPh group. Similar arguments for the meta and para protons lead to three sets of Ph ^{1}H NMR resonances being predicted for **2a** at ambient temperature, as is observed. At temperatures below −40 °C, rotation about the S–C_{Ph} bond is still rapid, but bridge–terminal exchange is now slow on the NMR time scale. The Ph aromatic resonances are harder to interpret in the ^{1}H NMR spectrum as the spin-coupled multiplets overlap each other, but the impact of slow bridge terminal exchange is clearly registered on the ^{13}C NMR spectrum of **2a**.

As free rotation about the S–C_{Ph} bonds should result in four distinct resonances for *each* Ph group in the ^{13}C NMR spectrum of **2a**, altogether eight Ph aromatic signals are expected (that correspond to the bridging and terminal μ-SPh groups). The seven signals actually seen for these carbon atoms suggest that the solid-state structure of **2a** is preserved in solution (it is likely that two resonances coincidentally overlap each other).

The NMR data available do not resolve the question of inversion at the sulfur atoms. For an effective mirror plane to exist in **2a**, either rapid inversion must occur or else the two SPh groups must remain locked in either the mutually anti conformation, that maximizes the angle between the two phenyl planes (as shown in Figure 3, the solid-state structure) or in a mutually syn conformation that minimizes this angle. Inversion at sulfur is not necessary to render the two phenyl groups equivalent as long as their conformation is maintained in solution, preserving the effective mirror plane. If inversion is ongoing, it must be rapid. There is no evidence of other conformational isomers present as only one set of η-C_5Me_5 and η-C_5H_4Me signals is seen in both the ^{13}C and ^{1}H NMR spectra of **2a** at all temperatures.

No VT NMR studies were carried out for complexes **2a′**, **2b**, **2c** and **2d**. However all these species show a similar effective mirror plane of symmetry on the NMR time scale at ambient temperatures. The comparable spectral IR and NMR spectral data for these species indicate that these complexes have analogous structures. The fluxional process described for **2a** is probably operational for all these species.

X-ray Structure of $[Ni(\eta\text{-}C_5Me_5)(\mu\text{-}SePh)]_2$ (3). The structure of **3** was confirmed by a single-crystal X-ray diffraction study. A labeled ORTEP diagram of **3** is shown in Figure 4. Cell and data collection parameters, atomic positional parameters, and key atomic distances and bond angles are gathered in Tables III, VI, and VII respectively.

Complex **3** has a crystallographically imposed center of symmetry and contains a planar Ni_2Se_2 rhomboidal core. The nickel atoms are not within bonding distance [Ni···Ni′ = 3.216(1) Å][21] and are bridged symmetrically by the SePh ligands. The two independent Ni–Se bonds, while not required to be so, are identical within their esd's at 2.301(1) Å. This span is significantly less than the value of 2.432(1) Å found for the Ni–μ-Se bonds in $[Ni(\mu\text{-}SePh)(SePh)(Me_2Phen)]_2$.[22] Other Ni–Se(aryl) distances for this and other related species[22] range from 2.340(2) to 2.605(1) Å, all significantly longer than the value seen in **3**.

The phenyl rings in **3** are practically at right angles (91.5°) to the Ni_2Se_2 plane and are close to parallel with the η-C_5Me_5 ring carbon atoms (the interplanar angle is 7.1°). The selenium atoms are pyramidal [the sum of angles around the Se atom is 296°; the value for the comparable μ-S atom in **2a** is 286°], and the phenyl groups, by virtue of the center of symmetry possessed by the molecule, are in an anti orientation with respect to each other.

Discussion

The unsaturated heterobimetallic complex **1** reacts with organic RE_2R (RE = SMe, SPh, SePh) species by oxidative addition of two RE fragments across the metal–metal bond. The metal atoms' formal oxidation states increase by one unit each [Ni(I) → Ni(II); W(I) → W(II)] on addition of the chalcogenide ligands. When one takes into account the different ligands and/or metals present, spectroscopic data for complexes **2** resemble each other closely: the data suggest that they are isostructural species with geometries similar to those of **2a**. All the reactions can be summarized by the following equation (the structures of the molecules are shown in Chart I).

$$\underset{\mathbf{1}}{(\eta\text{-}C_5Me_5)Ni\text{–}W(CO)_3(\eta\text{-}C_5H_4Me)} + RE_2R \rightarrow$$

$$\underset{\mathbf{2}}{(\eta\text{-}C_5Me_5)Ni(\mu\text{-}CO)(\mu\text{-}ER)W(CO)(ER)(\eta\text{-}C_5H_4Me)} +$$

[ER = SPh (**2a**), SePh (**2b**), SMe (**2c**)]

$$\underset{\substack{\mathbf{3}\\ \text{(only isolated}\\ \text{for ER = SePh)}}}{[(\eta\text{-}C_5Me_5)Ni(\mu\text{-}ER)]_2}$$

The complexes are fluxional and exhibit an effective mirror plane of symmetry on the NMR time scale. A dynamic process consistent with the NMR data is exchange of the bridging thiolato ligands with the terminal ones, coupled with exchange of the bridging carbonyl groups with the terminal carbonyl ligands. This process generates an effective mirror plane of symmetry in the molecule on the NMR time scale and is arrested at −80 °C. It requires that either the two SPh ligands must remain locked in a mutually syn or mutually anti conformation to maintain this mirror plane or else rapid inversion at both sulfur atoms must take place. Complexes in which there are both bridging and terminal thiolate groups occasionally are fluxional. The species $M_2(\mu\text{-}SEt)_6^{2-}$ (M = Zn, Cd, Ni, no metal–metal bonds) exhibit one set of ^{1}H NMR ethyl signals for M = Zn, Cd and two sets of such resonances for the dinickel anion.[17] No low-temperature

(21) This distance is short compared to other nonbonded Ni···Ni distances in related species. Values of 3.290(1)[16] and 3.355(2) Å[17] are found in anionic homoleptic $Ni_2(\mu\text{-}SR)_2(SR)_4^{2-}$ compounds. A very short nonbonded Ni···Ni distance of 2.607 Å has been noted in a $Ni_2(\mu\text{-}SR)_3(SR)_2]$ complex.[18]

(22) Baidya, N.; Noll, B. C.; Olmstead, M. M.; Mascharak, P. K. *Inorg. Chem.* **1992**, *31*, 2999.

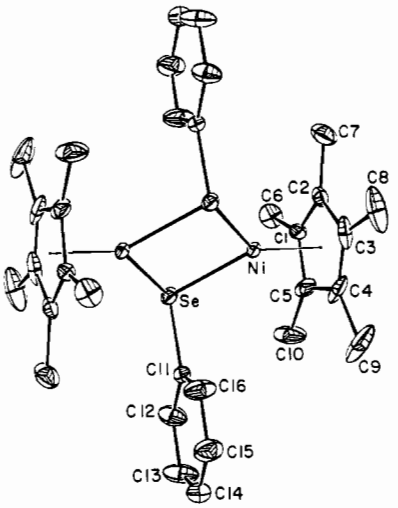

Figure 4. Labeled ORTEP plot of $[Ni(\eta\text{-}C_5Me_5)(\mu\text{-}SePh)]_2$ (**3**). Ellipsoids are shown at the 50% probability level; unlabeled atoms are symmetry related to the labeled atoms and are given the corresponding primed labels. Hydrogen atoms are not shown.

NMR data were reported for these species. The metal–metal bond present in **2a** may facilitate its SPh fluxionality.

Other multiply bonded species react with dialkyl disulfides via oxidative addition in an analogous fashion: the reaction of $[Mo(CO)_2(C_5H_5)]_2$ (Mo≡Mo) with Me_2S_2 affords mixtures of *cis*- and *trans*-$[Mo(\mu\text{-}SMe)(CO)(\eta\text{-}C_5H_5)]_2$ (Mo=Mo).[23] Interestingly, both thiolate ligands bridge the formal Mo=Mo double bond obtained in this case.

The structure of **2a** contains a bridging and a terminal μ-SPh ligand; steric congestion arising from the bulky pentamethylcyclopentadienyl ligand may allow only one large bridging ligand and thus may force one of the two benzenethiolate groups to become terminal. Complex **3** is analogous to other related $[Ni(\mu\text{-}ER)(\eta\text{-}L)]_2$ species (E = S, Se). Most of these contain a Ni_2E_2 core in which there are two unequal Ni–E distances. In contrast to the parallelogram-like Ni_2E_2 core frequently observed in such compounds, **3** contains a more symmetric rhomboid core in which all the Ni–E bonds are equal.

Dimethyl disulfide ruptures the metal–metal bond unless conditions are carefully controlled. Nevertheless, the other disulfide or diselenide ligands do not significantly cleave the unsaturated complexes into homometallic fragments under ambient conditions (small quantities of $[(\eta\text{-}C_5Me_5)Ni(\mu\text{-}SePh)]_2$ were recovered from the reaction of $PhSe_2Ph$ with **1**). The lack of reactivity of Me_2S with **1** is somewhat surprising in view of the affinity of both nickel and tungsten for sulfur.

Conclusion

Disulfides and diselenides react with the complexes $(\eta\text{-}C_5Me_5)Ni\text{–}M(CO)_3(\eta\text{-}C_5H_4Me)$ (**1**) (M = W, Mo) by cleavage of the RE–ER bonds and oxidative addition of two RE fragments to the molecule. In the ensuing species $(\eta\text{-}C_5Me_5)Ni(\mu\text{-}CO)(\mu\text{-}ER)M(CO)(ER)(\eta\text{-}C_5H_4Me)$ (Ni–M: M = W, ER = SPh, SMe, SePh; M = Mo, ER = SPh), only one of the chalcogenide ligands bridges the metals. The molecules contain a metal–metal single bond. Small quantities of $[Ni(\eta\text{-}C_5Me_5)(\mu\text{-}SePh)]_2$ were also isolated from the reaction of $PhSe_2Ph$ with **1**. Further investigations into the chemistry of **1** with chalcogenide-containing ligands are in progress.

Experimental Section

(i) General Remarks. All manipulations were carried out by using Schlenk or vacuum line techniques under a nitrogen atmosphere. Solvents were predried over 4-Å molecular sieves and were distilled over sodium benzophenone ketyl (diethyl ether and hexanes) or CaH_2 (dichloromethane). Deuterated NMR solvents were subjected to three freeze–pump–thaw cycles, and stored under an atmosphere of nitrogen prior to use. The reagents MeS_2Me, PhS_2Ph and $PhSe_2Ph$ were purchased from Aldrich and used as received. Syntheses of **1** and **1′** have been described.[6]

NMR spectra were obtained on General Electric NT-300 and GN-300 spectrometers at 20 °C in chloroform-d_1 unless otherwise stated. Low-temperature spectra for **2a** were obtained using acetone-d_6 as the solvent. $Cr(acac)_3$ (0.01–0.05 M) was added to ^{13}C NMR samples as a shiftless relaxation reagent. The $^{77}Se\{^1H\}$ NMR spectrum of **2b** was obtained from a chloroform-d_1 solution of **2b** using $PhSe_2Ph$ as an external reference. A total of 14 000 transients were collected using a spectrometer frequency of 57.3 MHz and a sweep width of ±11 111 Hz, and resulted in a signal with an S/N ratio of ≈5.5:1. IR spectra were recorded on an IBM IR-32 FT instrument, using the solvent-subtract function for solution samples. Elemental analyses were performed by M-H-W Labs, Phoenix, AZ. Mass spectra were obtained on a Finnegan-Matt instrument operating in the FAB mode. All parent ions show the appropriate isotopomer pattern. All the new species reported here are slightly soluble in hexanes and are moderately soluble in dichloromethane, chloroform-d_1, and diethyl ether. They are somewhat air-sensitive in solution, but appear to be stable in the solid state in air.

(ii) Attempted Reaction of Me_2S with $(\eta\text{-}C_5Me_5)Ni\text{–}W(CO)_3(\eta\text{-}C_5H_4Me)$ (1). Complex **1** (200 mg, 0.37 mmol) was dissolved in toluene (20 mL), and Me_2S (0.1 mL, ≈2 mmol) was added. No reaction ensued at 0 °C. The reaction was stirred overnight at ambient temperature but the deep blue color of **1** was not discharged. **1** was recovered unchanged from the reaction.

(iii) Synthesis of $(\eta\text{-}C_5Me_5)Ni(\mu\text{-}CO)(\mu\text{-}SPh)W(CO)(SPh)(\eta\text{-}C_5H_4Me)$ (Ni–W, 2a). Complex **1** (470 mg, 0.87 mmol) was dissolved in CH_2Cl_2 (25 mL) and chilled to −78 °C in an acetone/dry ice bath. A solution of PhS_2Ph (189 mg, 0.87 mmol) in 20 mL of CH_2Cl_2 was added dropwise over a 2-h period. The blue solution of **1** turned greenish brown after the addition was complete. Solvent was removed under reduced pressure and the solid material was washed with hexanes (washings were tan colored). The residue was recrystallized at −20 °C from a Et_2O/hexanes solution (1:1). Green crystals of $(\eta\text{-}C_5Me_5)Ni(\mu\text{-}CO)(\mu\text{-}SPh)W(CO)(SPh)(\eta\text{-}C_5H_4Me)$ (Ni–W, **2a**) were harvested in moderate yield (250 mg, 0.35 mmol, 40%). MS (FAB, *m/e*): 730, $(M)^+$; 702, $(M - CO)^+$; 674, $(M - 2CO)^+$; 621, $(M - SPh)^+$; 597, $(M - 2CO - Ph)^+$.

(iv) Synthesis of $(\eta\text{-}C_5Me_5)Ni(\mu\text{-}CO)(\mu\text{-}SPh)Mo(CO)(SPh)(\eta\text{-}C_5H_4Me)$ (Ni–Mo, 2a′). The complex $(\eta\text{-}C_5Me_5)Ni\text{–}Mo(CO)_3(\eta\text{-}C_5H_4Me)$ (Ni–Mo, **1a′**) (350 mg, 0.65 mmol) was dissolved in Et_2O (25 mL) and cooled to −78 °C. PhS_2Ph (141 mg, 0.65 mmol) in CH_2Cl_2 (15 mL) was added slowly to the solution of **1′**. After allowing the resulting brown solution to stir for 1 h, the mixture was taken to dryness. The product was rinsed with hexanes leaving behind a dark green solid. Recrystallization from Et_2O/hexanes at −20 °C afforded **2a′** in good yield (280 mg, 0.59 mmol, 60%). MS (FAB, *m/e*): 644, $(M)^+$; 616, $(M - CO)^+$; 606; 588 $(M - 2CO)^+$.

(v) Synthesis of $(\eta\text{-}C_5Me_5)Ni(\mu\text{-}CO)(\mu\text{-}SePh)W(CO)(SePh)(\eta\text{-}C_5H_4Me)$ (Ni–W, 2b) and $[(\eta\text{-}C_5Me_5)Ni(\mu\text{-}SePh)]_2$ (3). A solution of $PhSe_2Ph$ (231 mg, 0.74 mmol) in Et_2O was slowly added to an ethereal solution of **1** (400 mg, 0.74 mmol) at −78 °C. The blue solution immediately turned brown. The mixture was taken to dryness and separated into soluble and insoluble hexanes portions. The hexanes soluble portion was recrystallized at −20 °C from hexanes to afford **3** (30 mg, 0.043 mmol). The hexanes insoluble portion was dissolved in Et_2O, concentrated, layered with hexanes and placed in a −20 °C freezer. Recrystallization afforded **2b** as a black powder (366 mg, 0.44 mmol, 60%). MS for **2a** (FAB, *m/e*): 826, $(M)^+$; 798, $(M - CO)^+$; 770, $(M - 2CO)^+$; 693, $(M - 2CO - Ph)^+$; 669, $(M - SePh)^+$. MS for **3** (FAB, *m/e*): 700, $(M)^+$.

(vi) Synthesis of $(\eta\text{-}C_5Me_5)Ni(\mu\text{-}CO)(\mu\text{-}SMe)W(CO)(SMe)(\eta\text{-}C_5H_4Me)$ (Ni–W, 2c). **1** (520 mg, 0.96 mmol) was dissolved in Et_2O (30 mL) and cooled to −78 °C. A solution of MeS_2Me solution of MeS_2Me (0.087 mL, 0.96 mmol) in Et_2O (10 mL) was added slowly. The blue solution immediately turned greenish-brown. The reaction mixture was then taken to dryness under reduced pressure and rinsed with hexanes. The residue was dissolved in Et_2O, filtered, concentrated, layered with hexanes and placed in a freezer at −20 °C. Green crystals of **2c** were harvested (150 mg, 0.25 mmol, 26%). MS (FAB, *m/e*): 606, $(M)^+$; 578, $(M - CO)^+$; 550, $(M - 2CO)^+$; 531, $(M - SMe)^+$.

(vii) X-ray Diffraction Studies. (a) Structure of 2a. A dark green chunk of **2a**, grown from a diethyl ether/hexanes solution at −20 °C, was mounted in a glass capillary tube and placed on an Enraf-Nonius CAD

(23) Li, P.; Curtis, M. D. *Inorg. Chem.* **1990**, *29*, 1242.

4 Diffractometer at 20 ● 1 °C. Cell constants and an orientation matrix were obtained from least-squares refinement of 25 reflections in the range $15° \leq \theta \leq 20°$. The systematic absences indicated the space group was $P2_1/c$, and least-squares refinement was successful in this space group.

Data were corrected for Lorentz and polarization effects and an empirical absorption correction was applied.[24] Of the 3962 unique reflections, 2579 with $I > 3\sigma(I)$ were used in refinement. The structure was solved on a VAX computer using SDP/VAX software and the SHELX-86 solution package. Remaining atoms were located from succeeding Fourier maps; hydrogen atoms, located and added to the structure factor calculations, were not refined. Scattering factors were obtained from Cromer and Waber.[25] Anomalous dispersion effects were included in F_c.[26] The highest peak in the difference Fourier had a height of 0.65 e/Å^3 (estimated error based on $\Delta F = 0.10$).

(b) Structure of 3. Data are as for **2a** except as noted. A black crystal of **3**, grown from diethyl ether/hexanes solution at −20 °C, was mounted on a glass capillary tube and placed on an Enraf-Nonius CAD 4 diffractometer at −147 ● 2 °C. Least-squares refinement of 25 reflections in the range $8° \leq \theta \leq 21°$ led to the cell constants and an orientation matrix. No systematic absences were noted; subsequent successful least squares refinement indicated that the space group was $P\bar{1}$.

Of the 4018 unique reflections, 3223 with $I > 1.5\ \sigma(I)$ were used in refinement. A semiempirical absorption correction (ψ-curve method) was applied. Patterson maps were used to locate heavy atoms and remaining atoms were located from succeeding Fourier maps. The highest peak in the final difference Fourier had a height of 2.8 e/Å^3 (estimated error based on $\Delta F = 0.20$).

Acknowledgment. We gratefully acknowledge financial support from the American Chemical Society administered Petroleum Research Fund and from the University of Notre Dame.

Supplementary Material Available: Full tables of data collection parameters, positional parameters, bond lengths, bond angles, positional parameters for hydrogen atoms, and thermal parameters for all atoms of complexes **2a** and **3** (18 pages). Ordering information is given on any current masthead page.

(24) Walker, N.; Stuart, D. *Acta Crystallogr.* **1983**, *A39*, 158.
(25) Cromer, D. T.; Waber, J. T. *International Tables for X-ray Crystallography*, Kynoch Press: Birmingham, England, 1974; Vol. IV, Table 2.2B.
(26) (a) Ibers, J. A.; Hamilton, W. C. *Acta Crystallogr.* **1964**, *17*, 781. (b) Reference 25, Table 2.3.1.